A magnetoelastic theoretical model for soft ferromagnetic shell in magnetic field

Xiaojing Zheng [*], Xingzhe Wang

Department of Mechanics, Lanzhou University, Tianshui Road 298, Lanzhou 730000, PR China

Abstract

With the aid of a generalized variational method, in this paper, a theoretical model for soft ferromagnetic shells is derived to describe their magnetoelastic behavior in an applied magnetic field. Having made a quantitative comparison between the numerical predictions given by several theoretical models and the experimental results on strains of a cylindrical shell, we find that the predictions got by our model are in good agreement with the experimental data. It is also found that the Moon's model is a special case of the model derived in this paper when the relative magnetic permeability $\mu_r > 10^4$, which confirms that it is reasonable for the Moon's model to calculate strains of the soft ferromagnetic shells. Having displayed the distribution of the equivalent magnetic force in the length of the cylindrical shell and its circumferential bending strains with different elastic end constraints, we give an explanation for the discrepancy between Moon's analytical results and his experimental ones.
© 2003 Elsevier Ltd. All rights reserved.

Keywords: Ferromagnetic shells; Magnetoelastic interaction; Theoretical model; Numerical analysis

1. Introduction

There are many devices made of soft ferromagnetic materials and worked in electromagnetic field, such as fusion reactors, magnetically levitated vehicles and magnetic forming devices. When a ferromagnetic structure is placed in a magnetic field, it will be magnetized, and then deformed under a magnetic force system arisen from the magnetization. In general, the deformation of the ferromagnetic structure will also influence the magnetic force system subjected on the structure. It is complicated to describe this kind of coupled magnetoelastic problem since the magnetic force on the structure cannot be directly measured and this coupled problem is inherently nonlinear.

Moon and Pao (1969) firstly found that when a ferromagnetic beam-plate is in a transverse magnetic field, the natural frequency of the plate decreases with an increasing magnetic-field intensity and becomes

[*] Corresponding author. Tel.: +869318912112; fax: +869318625576.
E-mail address: xjzheng@lzu.edu.cn (X. Zheng).

near zero as the field attains a critical value, which causes the same plate to buckle statically. Twenty-four years later, Takagi et al. (1993) conducted another interesting experiment and found that when a ferromagnetic beam-plate is in an in-plane magnetic field, the natural frequency of the plate increases with an increasing magnetic-field intensity. There exist several famous theoretical models in magnetoelasticity, such as the Pao and Yeh's model (1973), the Eringen and Maugin's model (1990) as well as the Moon and Pao's model (1968). These models can qualitatively predict the Moon–Pao's experiment of the plate in a transverse magnetic field. However, Zhou and Miya (1998) found that when these models are used to describe the Takagi et al.'s experiment (1993) of the beam-plate in an in-plane magnetic field, the predicted natural frequency of the plate decreases. It states that all existing theoretical models are not suitable to describe the magnetoelastic behavior of the plate in an in-plane magnetic field. Zhou and Miya subsequently suggested a new theoretical model so that the Tagaki et al.'s experiment is qualitatively simulated well. For a ferromagnetic plate in complex magnetic fields, Zhou and Zheng (1997) derived a general expression of the magnetic force which was used by Zheng et al. (1999) to describe the bending and buckling of a rectangular ferromagnetic plate in an oblique magnetic field.

Besides the researches on ferromagnetic plates, soft ferromagnetic shells have also been paid more attention to since the shell is often used to shield a volume containing sensitive electronic equipment from magnetic field. Moon (1984) experimentally displayed that a thin, soft ferromagnetic cylindrical shell supported at its ends by circular nylon plates could produce bending in a uniform magnetic field. He analyzed that a distribution of body couples acts to bend the shell and calculated the magnetic forces with magnetic tension as they exert on the rigid and infinite cylindrical shell. An expression of the solution was obtained to predict stresses and strains of the cylindrical shell. However, there exist some discrepancies between the theoretical results and the experimental data. For example, the predicted maximum stress at 0.05 T was 990 N/cm^2 and the measured stress was 520 N/cm^2. Moon (1984) suggested that "more-refined experiments as well as more sophisticated shell analysis, taking into account the finite-length and end constraints, are need to assess the accuracy of the analytical method." Miyata and Miya (1988) conducted a similar experiment, in which a tube was in an applied magnetic field and was supported with fixed condition at both ends. They also gave some numerical results by the body pole model in which the shell experiences only the torque. Their numerical results are lower than their measured data, the maximum relative discrepancy is about 40%.

In this paper, a variational principle for soft ferromagnetic shells is suggested and an expression of the magnetic force subjected on the shell is derived. The finite element method is adopted to respectively calculate the deformation of a finite-length cylindrical shell and the magnetic fields in and out of the shell. The numerical simulation on the Miyata and Miya's experiment shows that the predicted results are in good agreement with the experimental data. In addition, the expression of the magnetic force suggested by Moon (1984) is confirmed to be a special case involved in our theoretical model. Having analyzed the effect of an elastic constant of the end constraints on the stresses of the cylindrical shell, we find that the difference between the actual end constraints and Moon's idealized treatment may be main reason which leads to the discrepancies between Moon's predicted results and his measured ones.

2. Fundamental equations

In this section, we first give out an expression of a total energy functional for a soft ferromagnetic thin shell in a magnetic field. Then, the first-order variation of the energy functional is derived and an expression of the magnetic force subjected on the shell is obtained. Finally, two sets of fundamental governing equations are respectively established for the shell and the magnetic fields in and out of the shell.
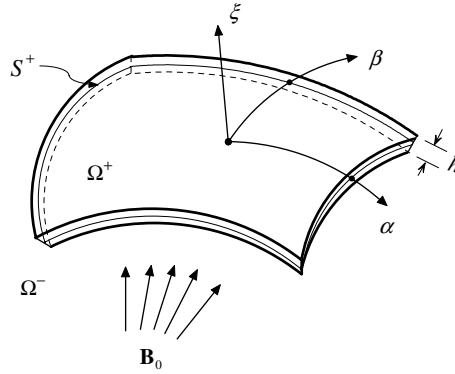
Fig. 1. Sketch of ferromagnetic shell in applied magnetic filed.

2.1. Energy functional

Consider a thin soft ferromagnetic shell with thickness h placed in a stationary magnetic field $\mathbf{B}_0$, without electric field, charge distribution and conducting current on and in the shell (as shown in Fig. 1). For linear, homogeneous and isotropic magnetic materials, we have the magnetic constitutive relationships as follows

$$\mathbf{M}^+ = \chi_m \mathbf{H}^+ \quad \text{in } \Omega^+ \tag{1}$$

$$\mathbf{B}^+ = \mu_0 \mu_r \mathbf{H}^+ \quad \text{in } \Omega^+ \tag{2}$$

$$\mathbf{M}^- = \mathbf{0} \quad \text{in } \Omega^- \tag{3}$$

$$\mathbf{B}^- = \mu_0 \mathbf{H}^- \quad \text{in } \Omega^- \tag{4}$$

in which Ω^+ and Ω^- are the inside and outside region of the shell, respectively; $\mathbf{M}^+$ and $\mathbf{M}^-$ are respectively the magnetization vectors in the shell and in vacuum; $\mathbf{B}^+$, $\mathbf{H}^+$, and $\mathbf{B}^-$ as well as $\mathbf{H}^-$ are the magnetic induction intensity vectors and magnetic intensity vectors inside and outside the shell; μ_r and μ_0 are the magnetic permeability in the shell and in vacuum, respectively; χ_m is the susceptibility of the ferromagnetic shell and $\chi_m = \mu_r - 1$.

Taking $\mathbf{u} = \{u, v, w\}$ as the displacement vector of thin shell, S_0 as a surface which encloses and is far away from the region of the ferromagnetic shell, we can write the magnetic-energy functional for the system as follows

$$\Pi_1\{\phi, \mathbf{u}\} = \frac{1}{2} \int_{\Omega^+(\mathbf{u})} \mu_0 \mu_r (\nabla \phi^+)^2 \, dv + \frac{1}{2} \int_{\Omega^-(\mathbf{u})} \mu_0 (\nabla \phi^-)^2 \, dv + \int_{S_0} \mathbf{n} \cdot \mathbf{B}_0 \phi^- \, ds \tag{5}$$

where ϕ is a magnetic scalar potential which satisfies $-\nabla \phi = \mathbf{H}$, ∇ is a 3D gradient operator (i.e., $\nabla = \partial/\partial x \mathbf{i} + \partial/\partial y \mathbf{j} + \partial/\partial z \mathbf{k}$, in which $\mathbf{i}$, $\mathbf{j}$, and $\mathbf{k}$ are unit vectors along the x-, y-, and z-axis, respectively).

When external mechanical forces on the ferromagnetic shell and the effect of shear deformation of the shell are neglected, the mechanical strain energy for the system can be expressed as

$$\begin{aligned}
\Pi_2\{\phi, \mathbf{u}\} &= \frac{1}{2} \int_{\Omega^+} (\varepsilon_\alpha \sigma_\alpha + \varepsilon_\beta \sigma_\beta + \varepsilon_{\alpha\beta} \sigma_{\alpha\beta}) \, dv \\
&= \frac{1}{2} \int_{S^+} \left\{ C \left[\varepsilon_\alpha^2 + \varepsilon_\beta^2 + 2v\varepsilon_\alpha \varepsilon_\beta + \frac{1}{2}(1-v)\varepsilon_{\alpha\beta}^2 \right] + D[\chi_\alpha^2 + \chi_\beta^2 + 2v\chi_\alpha\chi_\beta + (1-v)\chi_{\alpha\beta}^2] \right\} ds
\end{aligned} \tag{6}$$

in which α, β are principal curvature lines on the middle surface S^+ of the thin shell (as shown in Fig. 1); $C = Yh/1 - v^2$ and $D = Yh^3/12(1 - v^2)$ are the tensile rigidity and the flexural rigidity of the shell, respectively; Y is the Young's modulus, v the Poisson's ratio, h the thickness of the shell; $\{\varepsilon_\alpha, \varepsilon_\beta, \varepsilon_{\alpha\beta}, \chi_\alpha, \chi_\beta, \chi_{\alpha\beta}, \sigma_\alpha, \sigma_\beta, \sigma_{\alpha\beta}\}$ are respectively the strains and stresses of the thin shell (Timoshenko and Woinowsky-Krieger, 1959).

The total energy functional of the magnetoelastic system can be obtained by adding Π_1 for the magnetic energy and Π_2 for the elastic strain energy. That is

$$\Pi\{\phi, \mathbf{u}\} = \Pi_1\{\phi, \mathbf{u}\} + \Pi_2\{\phi, \mathbf{u}\} \tag{7}$$

2.2. Generalized variational principle

Here, we take $\delta\phi$ as one admissible variation on magnetic potential function of the system and $\delta\mathbf{u}$ as another admissible variation on displacement of the shell. It is obvious that we have

$$\delta\phi = \delta\phi^+ = \delta\phi^- \quad \text{on } S \tag{8}$$

$$\delta\mathbf{u} = \mathbf{0} \quad \text{on } C_u \tag{9}$$

in which S is the enclosed surface of the shell region Ω^+; C_u denotes the boundary of the shell on which displacements are known. By a generalized variational principle of magnetoelastic system, we have

$$\delta\Pi\{\phi, \mathbf{u}\} = \delta_\phi \Pi\{\phi, \mathbf{u}\} + \delta_{\mathbf{u}} \Pi\{\phi, \mathbf{u}\} \tag{10}$$

where

$$\delta_\phi \Pi\{\phi, \mathbf{u}\} = -\int_{\Omega^+(\mathbf{u})} \mu_0 \mu_r (\nabla^2 \phi^+) \delta\phi^+ \, dv - \int_{\Omega^-(\mathbf{u})} \mu_0 (\nabla^2 \phi^-) \delta\phi^- \, dv + \oint_S \mu_0 \left[\mu_r \frac{\partial \phi^+}{\partial n} - \frac{\partial \phi^-}{\partial n} \right] \delta\phi \, ds$$
$$+ \int_{S_0} \mathbf{n} \cdot [\mu_0 \nabla \phi^- + \mathbf{B}_0] \delta\phi^- \, ds \tag{11}$$

and

$$\delta_{\mathbf{u}} \Pi\{\phi, \mathbf{u}\} = -\int_{S^+} \frac{1}{AB} \left\{ \left[\frac{\partial}{\partial \alpha}(BN_\alpha) - N_\beta \frac{\partial B}{\partial \alpha} + \frac{\partial}{\partial \beta}(AN_{\alpha\beta}) + N_{\alpha\beta} \frac{\partial A}{\partial \beta} \right] \delta u + \left[\frac{\partial}{\partial \beta}(AN_\beta) - N_\alpha \frac{\partial A}{\partial \beta} \right. \right.$$
$$+ \frac{\partial}{\partial \alpha}(BN_{\alpha\beta}) + N_{\alpha\beta} \frac{\partial B}{\partial \alpha} \right] \delta v + \left[\frac{\partial}{\partial \alpha} \frac{1}{A} \left(\frac{\partial}{\partial \alpha}(BM_\alpha) + \frac{\partial}{\partial \beta}(AM_{\alpha\beta}) + \frac{\partial A}{\partial \beta} M_{\alpha\beta} - \frac{\partial B}{\partial \alpha} M_\beta \right) \right.$$
$$\left. + \frac{\partial}{\partial \beta} \frac{1}{B} \left(\frac{\partial}{\partial \beta}(AM_\beta) + \frac{\partial}{\partial \alpha}(BM_{\alpha\beta}) + \frac{\partial B}{\partial \alpha} M_{\alpha\beta} - \frac{\partial A}{\partial \beta} M_\alpha \right) - AB \left(\frac{N_\alpha}{R_\alpha} + \frac{N_\beta}{R_\beta} \right) \right] \delta w \right\} ds$$
$$+ \frac{1}{2} \int_{S^+} [\mu_0 \mu_r (\mathbf{H}^+)^2 - \mu_0 (\mathbf{H}^-)^2]_{\xi=-h/2}^{\xi=h/2} \delta w \, ds + \left\{ \int_{C_u} \cdots + \int_{C_t} \cdots \right\} \tag{12}$$

where A and B are respectively the Lame's constants along the directions of α and β, R_α and R_β are the principal curvature radii, respectively; $\{\int_{C_u} \cdots + \int_{C_t} \cdots\}$ means the integration associated with the displacement and stress boundary conditions of the shell; N_α, N_β, $N_{\alpha\beta}$ and M_α, M_β, $M_{\alpha\beta}$ respectively represent membrane stress and bending stress resultants of the thin shell and are defined by

$$N_\alpha = C(\varepsilon_\alpha + v\varepsilon_\beta), \quad N_\beta = C(\varepsilon_\beta + v\varepsilon_\alpha), \quad N_{\alpha\beta} = \frac{C}{2}(1 - v)\varepsilon_{\alpha\beta} \tag{13}$$

$$M_\alpha = D(\chi_\alpha + v\chi_\beta), \quad M_\beta = D(\chi_\beta + v\chi_\alpha), \quad M_{\alpha\beta} = D(1 - v)\chi_{\alpha\beta} \tag{14}$$

Having considered jumping conditions of the magnetic field on the surface of the ferromagnetic shell, that is

$$\mathbf{n} \cdot (\mathbf{B}^+ - \mathbf{B}^-) = 0, \quad \mathbf{n} \times (\mathbf{H}^+ - \mathbf{H}^-) = \mathbf{0} \quad \text{on } S \tag{15}$$

or

$$H_n^- = \mu_{\mathrm{r}} H_n^+, \quad B_\tau^- = \frac{1}{\mu_{\mathrm{r}}} B_\tau^+ \quad \text{on } S \tag{16}$$

an expression of the equivalent magnetic force exerted on the shell $q_\xi^{\mathrm{em}}(\alpha, \beta)$, which can be regarded as a transformation from the magnetic energy to the mechanical energy of the system, is obtained by

$$q_\xi^{\mathrm{em}}(\alpha, \beta) = \frac{\mu_0 \mu_{\mathrm{r}} \chi_m}{2} \{[\mathbf{H}_n^+(\alpha, \beta, h/2)]^2 - [\mathbf{H}_n^+(\alpha, \beta, -h/2)]^2\} - \frac{\mu_0 \chi_m}{2} \{[\mathbf{H}_\tau^+(\alpha, \beta, h/2)]^2$$
$$- [\mathbf{H}_\tau^+(\alpha, \beta, -h/2)]^2\} \tag{17}$$

where ξ denotes the normal direction of the shell middle surface, together with α and β to constitute an orthogonal curvilinear coordinate system; $\mathbf{H}_n^+$ and $\mathbf{H}_\tau^+$ are the normal and tangential component vectors of magnetic field $\mathbf{H}^+(= \mathbf{H}_n^+ + \mathbf{H}_\tau^+)$ on the surface S.

2.3. Fundamental governing equations

By $\delta\Pi\{\phi, \mathbf{u}\} = 0$, one can derive all fundamental equations and boundary conditions for a ferromagnetic shell in an applied magnetic field $\mathbf{B}_0$ as follows
Governing equations for magnetic field

$$\nabla^2 \phi^+ = 0 \quad \text{in } \Omega^+(\mathbf{u}) \tag{18a}$$

$$\nabla^2 \phi^- = 0 \quad \text{in } \Omega^-(\mathbf{u}) \tag{18b}$$

with jumping conditions

$$\phi^+ = \phi^-, \quad \mu_{\mathrm{r}} \frac{\partial \phi^+}{\partial n} = \frac{\partial \phi^-}{\partial n} \quad \text{on } S \tag{18c}$$

and the boundary condition

$$-\nabla \phi^- = \frac{1}{\mu_0} \mathbf{B}_0 \quad \text{at } \infty \text{ or on } S_0 \tag{18d}$$

Equilibrium equations for thin shell

$$\frac{\partial}{\partial \alpha}(BN_\alpha) + \frac{\partial}{\partial \beta}(AN_{\alpha\beta}) + \frac{\partial A}{\partial \beta} N_{\alpha\beta} - \frac{\partial B}{\partial \alpha} N_\beta = 0 \tag{19a}$$

$$\frac{\partial}{\partial \beta}(AN_\beta) + \frac{\partial}{\partial \alpha}(BN_{\alpha\beta}) + \frac{\partial B}{\partial \alpha} N_{\alpha\beta} - \frac{\partial A}{\partial \beta} N_\alpha = 0 \tag{19b}$$

$$-\frac{\partial}{\partial \alpha} \frac{1}{A}\left[\frac{\partial}{\partial \alpha}(BM_\alpha) + \frac{\partial}{\partial \beta}(AM_{\alpha\beta}) + \frac{\partial A}{\partial \beta} M_{\alpha\beta} - \frac{\partial B}{\partial \alpha} M_\beta\right] - \frac{\partial}{\partial \beta} \frac{1}{B}\left[\frac{\partial}{\partial \beta}(AM_\beta) + \frac{\partial}{\partial \alpha}(BM_{\alpha\beta}) + \frac{\partial B}{\partial \alpha} M_{\alpha\beta} - \frac{\partial A}{\partial \beta} M_\alpha\right]$$
$$+ AB\left(\frac{N_\alpha}{R_\alpha} + \frac{N_\beta}{R_\beta}\right) = ABq_\xi^{\mathrm{em}}(\alpha, \beta) \tag{19c}$$

the boundary conditions on displacements and stresses of the shell can be obtained from the term $\{\int_{C_u} \cdots + \int_{C_t} \cdots\}$ in Eq. (12).

It should be noted from Eqs. (18a) and (18b) that the magnetic-field distribution of the shell is depended on the deformation **u** of the shell. On the other hand, the equivalent magnetic force exerted on the shell is depended on the magnetic-field distribution. So the magnetic-field distribution and the deformation of the ferromagnetic shell are coupled and influenced each other. In this case, the magnetoelastic problem is nonlinear even if the linear theory for magnetic materials and the shell is adopted.

3. Analyses and reviews on several models

There are lots of theoretical models which can be used to describe the magnetoelastic behavior of ferromagnetic structures. Some of them are famous, such as the Pao–Yeh's model, the Eringen–Maugin's model, and the Moon–Pao's model. From these models, the corresponding expressions of equivalent magnetic forces exerted on ferromagnetic structures are derived to predict magnetoelastic behavior of ferromagnetic structures. Zhou and Zheng (1997) found that all of them can qualitatively simulate the Moon's experiment (1968) of magnetoelastic buckling well, but cannot be used for the Takagi et al. one(1993). Here, we will firstly verify that the model suggested in this paper, by generated to the ferromagnetic plate in applied magnetic fields, is suitable to simulate not only the Moon's experiment, but also the Tagaki et al.'s one. Then, the equivalent magnetic force system by other models are derived for a thin ferromagnetic shell, and the distribution of the magnetic forces from these models to show the differences among these existing theoretical models is furthermore displayed. Finally, a discussion about the Moon's model (1984) is given to demonstrate that it is a special case of the model given in this paper when $\mu_r > 10^4$.

3.1. The model in this paper

In our model, the equivalent magnetic force (only in normal direction ξ) subjected on the middle surface of the shell is given by Eq. (17). Once we use it for a soft ferromagnetic plate, it will be rewritten as follows

$$q_\xi^{em}(x,y) = \frac{\mu_0\mu_r\chi_m}{2}\{[\mathbf{H}_n^+(x,y,h/2)]^2 - [\mathbf{H}_n^+(x,y,-h/2)]^2\} - \frac{\mu_0\chi_m}{2}\{[\mathbf{H}_\tau^+(x,y,h/2)]^2$$
$$- [\mathbf{H}_\tau^+(x,y,-h/2)]^2\} \tag{20}$$

where x, y represents the coordinate axes on the mid-plane of thin plate.

For a transverse magnetic field, we have $H_n^+ \gg H_\tau^+$, and the magnetic force acted on the plate is simplified as

$$q_\xi^{em}(x,y) = \frac{\mu_0\mu_r\chi_m}{2}\{[\mathbf{H}_n^+(x,y,h/2)]^2 - [\mathbf{H}_n^+(x,y,-h/2)]^2\} \tag{21a}$$

which is just same as the model suggested by Zhou and Zheng (1997) to predict the Moon and Pao's experiment (1968) not only in quality, but also in quantity well.

For an in-plane magnetic field, we have $H_\tau^+ \gg H_n^+$, so the magnetic force subjected on the plate becomes

$$q_\xi^{em}(x,y) = -\frac{\mu_0\chi_m}{2}\{[\mathbf{H}_\tau^+(x,y,h/2)]^2 - [\mathbf{H}_\tau^+(x,y,-h/2)]^2\} \tag{21b}$$

It is just the Zhou and Miya's model (1998), which can simulate the Tagaki et al.'s experiment, that is, the predicted natural frequency of ferromagnetic beam-plate increases with an increasing magnetic-field intensity. Consequently, when the model suggested in this paper is used for a ferromagnetic thin plate, it can simulate the magnetoelastic behavior of the plate not only in a transverse but also in an in-plane magnetic field.

3.2. The Moon–Pao's model

For a soft ferromagnetic thin plate, Moon and Pao (1968) neglected the magnetic field arisen from magnetization of the materials, and gave the magnetic body force $\mathbf{f}^{em}$ and body couple $\mathbf{c}$ as follows

$$\mathbf{f}^{em} = \mathbf{0}, \quad \mathbf{c} = \mathbf{M}^+ \times \mathbf{B}_0 \tag{22}$$

Having simplified the force system to the middle surface of the shell, we have the equivalent normal magnetic force

$$q_\xi^{em} = \int_{-h/2}^{h/2} [\nabla \times (\mathbf{M}^+ \times \mathbf{B}_0)] \cdot \mathbf{n}\, d\xi \tag{23a}$$

and tangential magnetic force

$$\mathbf{q}_\tau^{em} = \int_{-h/2}^{h/2} [\nabla \times (\mathbf{M}^+ \times \mathbf{B}_0)] \times \mathbf{n}\, d\xi \tag{23b}$$

3.3. The Pao–Yeh's model

Based on the Maxwell's stress tensor

$$\mathbf{T}^{em} = \mathbf{B}^+ \mathbf{H}^+ - \frac{1}{2}\mu_0 (\mathbf{H}^+ \cdot \mathbf{H}^+)\mathbf{I} \tag{24}$$

in which $\mathbf{I}$ is a unit matrix, Pao and Yeh (1973) derived the magnetic force system subjected on a ferromagnetic body as follows

$$\mathbf{f}^{em} = \nabla \cdot \mathbf{T}^{em} = \frac{\mu_0 \chi_m}{2} \nabla (\mathbf{H}^+)^2 \quad \text{in } \Omega^+ \tag{25a}$$

$$\mathbf{F}_S^{em} = -\mathbf{n} \cdot [\mathbf{T}^{em}] = \frac{\mu_0}{2}(\chi_m \mathbf{H}_n^+)^2 \mathbf{n} \quad \text{on } S \tag{25b}$$

Once we simplify this force system to the middle surface of the shell, we have

$$\begin{aligned}
q_\xi^{em} &= \frac{\mu_0 \chi_m}{2} \int_{-h/2}^{h/2} \nabla (\mathbf{H}^+)^2 \cdot \mathbf{n}\, d\xi + \frac{\mu_0 \chi_m^2}{2} \{ [\mathbf{H}_n^+(\alpha, \beta, h/2)]^2 - [\mathbf{H}_n^+(\alpha, \beta, -h/2)]^2 \} \\
&= \frac{\mu_0 \mu_r \chi_m}{2} \{ [\mathbf{H}_n^+(\alpha, \beta, h/2)]^2 - [\mathbf{H}_n^+(\alpha, \beta, -h/2)]^2 \} + \frac{\mu_0 \chi_m}{2} \{ [\mathbf{H}_\tau^+(\alpha, \beta, h/2)]^2 \\
&\quad - [\mathbf{H}_\tau^+(\alpha, \beta, -h/2)]^2 \}
\end{aligned} \tag{26a}$$

and

$$\mathbf{q}_\tau^{em} = \frac{\mu_0 \chi_m}{2} \int_{-h/2}^{h/2} \nabla (\mathbf{H}^+)^2 \times \mathbf{n}\, d\xi \tag{26b}$$

3.4. The Eringen–Maugin's model

Eringen and Maugin (1990) chose the Maxwell's stress tensor in another form

$$\mathbf{T}^{em} = \mathbf{B}^+ \mathbf{H}^+ - \frac{1}{2}(\mathbf{B}^+ \cdot \mathbf{B}^+/\mu_0 - \mathbf{M}^+ \cdot \mathbf{B}^+)\mathbf{I} \tag{27}$$

so a corresponding magnetic force system is taken as

$$\mathbf{f}^{\mathrm{em}} = \nabla \cdot \mathbf{T}^{\mathrm{em}} = \frac{\mu_0 \mu_r \chi_m}{2} \nabla (\mathbf{H}^+)^2 \quad \text{in } \Omega^+ \tag{28a}$$

$$\mathbf{F}_S^{\mathrm{em}} = -\mathbf{n} \cdot [\mathbf{T}^{\mathrm{em}}] = -\frac{\mu_0}{2} (\chi_m \mathbf{H}_\tau^+)^2 \mathbf{n} \quad \text{on } S \tag{28b}$$

Having simplified this system to the middle surface of the shell, we have

$$
\begin{aligned}
q_\xi^{\mathrm{em}} &= \frac{\mu_0 \mu_r \chi_m}{2} \int_{-h/2}^{h/2} \nabla (\mathbf{H}^+)^2 \cdot \mathbf{n}\, \mathrm{d}\xi - \frac{\mu_0 \chi_m^2}{2} \{ [\mathbf{H}_\tau^+(\alpha, \beta, h/2)]^2 - [\mathbf{H}_\tau^+(\alpha, \beta, -h/2)]^2 \} \\
&= \frac{\mu_0 \mu_r \chi_m}{2} \{ [\mathbf{H}_n^+(\alpha, \beta, h/2)]^2 - [\mathbf{H}_n^+(\alpha, \beta, -h/2)]^2 + \frac{\mu_0 \chi_m}{2} \{ [\mathbf{H}_\tau^+(\alpha, \beta, h/2)]^2 - [\mathbf{H}_\tau^+(\alpha, \beta, -h/2)]^2 \}
\end{aligned}
\tag{29a}
$$

and

$$\mathbf{q}_\tau^{\mathrm{em}} = \frac{\mu_0 \mu_r \chi_m}{2} \int_{-h/2}^{h/2} \nabla (\mathbf{H}^+)^2 \times \mathbf{n}\, \mathrm{d}\xi \tag{29b}$$

3.5. The Moon's model

Moon (1984) gave an analytical solution to a cylindrical shell in a uniform magnetic field. He firstly determined the magnetic field distribution on the rigid cylindrical shell, and then calculated the magnetic force acted on it by

$$q_\xi^{\mathrm{em}} = \frac{1}{2\mu_0} \{ [\mathbf{B}_n^+(\alpha, \beta, h/2)]^2 - [\mathbf{B}_n^+(\alpha, \beta, -h/2)]^2 \} \tag{30}$$

which he called as magnetic tension. In fact, it is not difficult to find that Eq. (30) just means the magnetic pressure difference between the outer and the inner surface of the cylindrical shell, and also that we can get the magnetic pressure difference from Eq. (17) once the case $\mu_r H_n^+ \gg H_\tau^+$ is considered. By calculating and comparing the magnetic forces respectively from Eqs. (17) and (30), we find that there is almost no difference between two models for the case $\mu_r > 10^4$. Consequently, the Moon's model (1984) is just a special case of the model suggested in this paper (see Section 5).

4. Computation formulations

In order to calculate the deformation of a cylindrical shell with finite-length and end constraints in a uniform magnetic field, a computation program is suggested in this section. The finite element method is respectively used to get the deformation of the cylindrical shell and the magnetic-field distributions both in and out of the shell. An iterative method is used in the program to solve the nonlinearity arising from the interaction between the deformation and the magnetic fields.

4.1. FEM analysis for magnetic field

Here, we will numerically analyze the magnetic-field distribution in regions Ω^+ and Ω^- that are influenced, respectively, by the magnetization of the ferromagnetic cylindrical shell and its deformation. For a given deformation state of the shell, the magnetic field distribution, that is the solution of the Eqs. (18a)–

(18d), minimizes the functional of Eq. (5). One can discretize the 3D regions of Ω^+ and Ω^- into finite elements, and set the surface and the middle surface of the shell being located on the surface of the elements. Here the 3D 20-node hexahedral element is chosen. A typical mesh for the ferromagnetic shell region and outside region of the shell is shown in Fig. 3a. Having taken $[\mathbf{N}(x, y, z)]_e$ as a shape function, we can write the value of the magnetic potential ϕ in compact matrix form as follows

$$\phi(x, y, z) = [\mathbf{N}(x, y, z)]_e[\mathbf{\Phi}]_e \tag{31}$$

where $[\mathbf{\Phi}]_e$ is a column matrix which consists of the value of ϕ on each node of the element e. Integrating Eq. (5) in the subregion of each element, and substituting Eq. (31) into it, we can obtain

$$\Pi_1\{\phi, \mathbf{u}\} = \sum_e \frac{1}{2}[\mathbf{\Phi}]_e^{\mathrm{T}}[\mathbf{K}^{\mathrm{em}}]_e[\mathbf{\Phi}]_e - \sum_{e_0}[\mathbf{\Phi}]_{e_0}^{\mathrm{T}}[\mathbf{P}]_{e_0} \tag{32}$$

where e_0 is the element on S_0; $[\mathbf{K}^{\mathrm{em}}]_e$ is a magnetic stiffness matrix of the element e and $[\mathbf{P}]_{e_0}$ is a inhomogenous term on S_0, which are respectively in following forms

$$[\mathbf{K}^{\mathrm{em}}]_e = \begin{cases} \int_{\Omega_e} \mu_0\mu_{\mathrm{r}}[\nabla\mathbf{N}]_e^{\mathrm{T}}[\nabla\mathbf{N}]_e \, \mathrm{d}v & \Omega_e \in \Omega^+(\mathbf{u}) \\ \int_{\Omega_e} \mu_0[\nabla\mathbf{N}]_e^{\mathrm{T}}[\nabla\mathbf{N}]_e \, \mathrm{d}v & \Omega_e \in \Omega^-(\mathbf{u}) \end{cases} \tag{33a}$$

$$[\mathbf{P}]_{e_0} = -\int_{S_{e_0}} \mu_0\mathbf{n}\cdot\mathbf{B}_0[\mathbf{N}]_e^{\mathrm{T}} \, \mathrm{d}s \quad S_{e_0} \in S_0 \tag{33b}$$

From $\delta_\phi\Pi_1\{\phi, \mathbf{u}\} = 0$, the global stiffness equation for the magnetic field is achieved by the form

$$[\mathbf{K}^{\mathrm{em}}][\mathbf{\Phi}] = [\mathbf{P}] \tag{34}$$

Since the region $\Omega^+(\mathbf{u})$ or $\Omega^-(\mathbf{u})$ denotes the inside or outside region of the deformed ferromagnetic shell, the coordinates of a point in the region Ω^+ and on the surface S must be considered in the configuration of the deformed shell for calculations of Eq. (33a), the coordinates $\hat{\mathbf{x}} = \{\hat{x}, \hat{y}, \hat{z}\}$ for deformed shell is expressed by $\hat{\mathbf{x}} = \mathbf{x} + \mathbf{u}$, where $\mathbf{x} = \{x, y, z\}$ is the coordinates for unformed shell. Consequently, the magnetic rigidity matrix $[\mathbf{K}^{\mathrm{em}}]$ should be a function of the displacement $\mathbf{u}$, that is

$$[\mathbf{K}^{\mathrm{em}}] = [\mathbf{K}^{\mathrm{em}}(\mathbf{u})] \tag{35}$$

which states the effect of the deformation of the shell on the deformation of the magnetic field or the magnetic potential $\phi(x, y, z)$.

4.2. FEM analysis for deformation of cylindrical shell

For a ferromagnetic cylindrical shell as shown in Fig. 2, taking the areas of those 3D hexahedral elements in the middle surface of shell as the shell elements, that is, a kind of eight-node shell element is chosen for analysis of its deformation. The typical mesh of shell and the shell element are shown in Fig. 3b. We take the global coordinate at a node of a shell element e as (r_i, θ_i, z_i) $(i = 1, 2, \ldots, 8)$ and a local coordinate system for the element as $\{o\gamma\eta\zeta\}$. The displacements at each node of the element are denoted as $[U_i]_e = \{u_i, v_i, w_i, \omega_{iz}, \omega_{i\theta}\}$, which represent the displacements along the three axes and the rotations round the z-axis and θ-axis, respectively. Consequently, the displacements at an arbitrary point in the subregion of shell element can be expressed as

$$\mathbf{u} = [\mathbf{N}(\gamma, \eta, \zeta)]_e[\mathbf{U}]_e \tag{36}$$

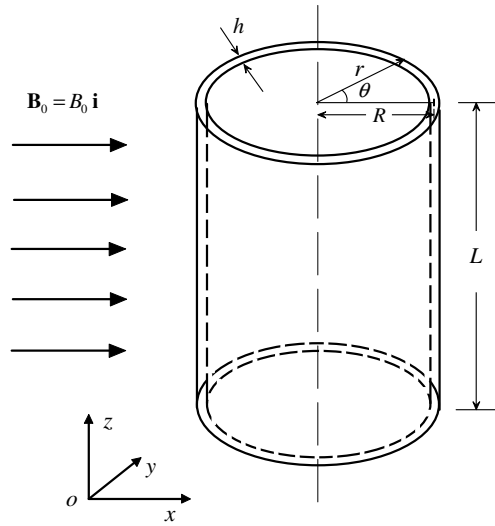where $[\mathbf{N}(\gamma, \eta, \zeta)]_e$ is the shape function.

Fig. 2. Sketch of a ferromagnetic cylindrical shell in a uniform magnetic field.

With the aid of the FEM, the deformation of the cylindrical shell governed by the differential Eqs. (19a)–(19c) with the corresponding boundary conditions can be reduced into a matrix equation

$$[\mathbf{K}^{me}][\mathbf{U}] = [\mathbf{Q}] \tag{37}$$

where $[\mathbf{K}^{me}]$ is the stiffness matrix for the deformation of the shell; $[\mathbf{U}]$ is a column matrix which consists of the displacements and rotations of each node on the middle surface of shell. $[\mathbf{Q}]$ is a column matrix related to the equivalent magnetic forces, it is obvious that $[\mathbf{Q}]$ is the function of $[\mathbf{\Phi}]$, that is

$$[\mathbf{Q}] = [\mathbf{Q}([\mathbf{\Phi}])] \tag{38}$$

4.3. Iterative arithmetic for nonlinearity

From Eqs. (34), (35) and (37), (38), we can get the following formula

$$[\mathbf{U}] = [\mathbf{K}^{me}]^{-1}[\mathbf{Q}([\mathbf{K}^{em}(\mathbf{u})]^{-1}[\mathbf{P}])] \tag{39}$$

To solve the above nonlinear equation, an iterative arithmetic (Zhou et al., 1996; Zheng et al., 1999) is employed and Eq. (39) will be taken as

$$[\mathbf{U}]_{m+1} = [\mathbf{K}^{me}]^{-1}[\mathbf{Q}([\mathbf{K}^{em}(\mathbf{u}_m)]^{-1}[\mathbf{P}])] \tag{40}$$

The iterative procedure is mainly shown as following. (i) Assuming an initial displacement $[\mathbf{U}]_0$ of shell for an applied magnetic field $\mathbf{B}_0$, with the interpolation function of Eq. (36) we can get the displacement $\mathbf{u}_0$ at the arbitrary point in the ferromagnetic medium, (ii) taking into account the effect $\mathbf{u}_0$ on the magnetic stiffness matrices and solving for magnetic field distribution $\mathbf{H}^+$, one can further calculate the magnetic force acted on the shell by Eq. (17), (iii) with the aid of solving Eq. (40), the new displacement $[\mathbf{U}]_1$ of shell will be gotten and (iv) having substituted $[\mathbf{U}]_1$ for the initial value $[\mathbf{U}]_0$ and repeating above procedure until a pre-specified precision condition

$$\|[\mathbf{U}]_{m+1} - [\mathbf{U}]_m\|/\|[\mathbf{U}]_m\| < \varepsilon \tag{41}$$
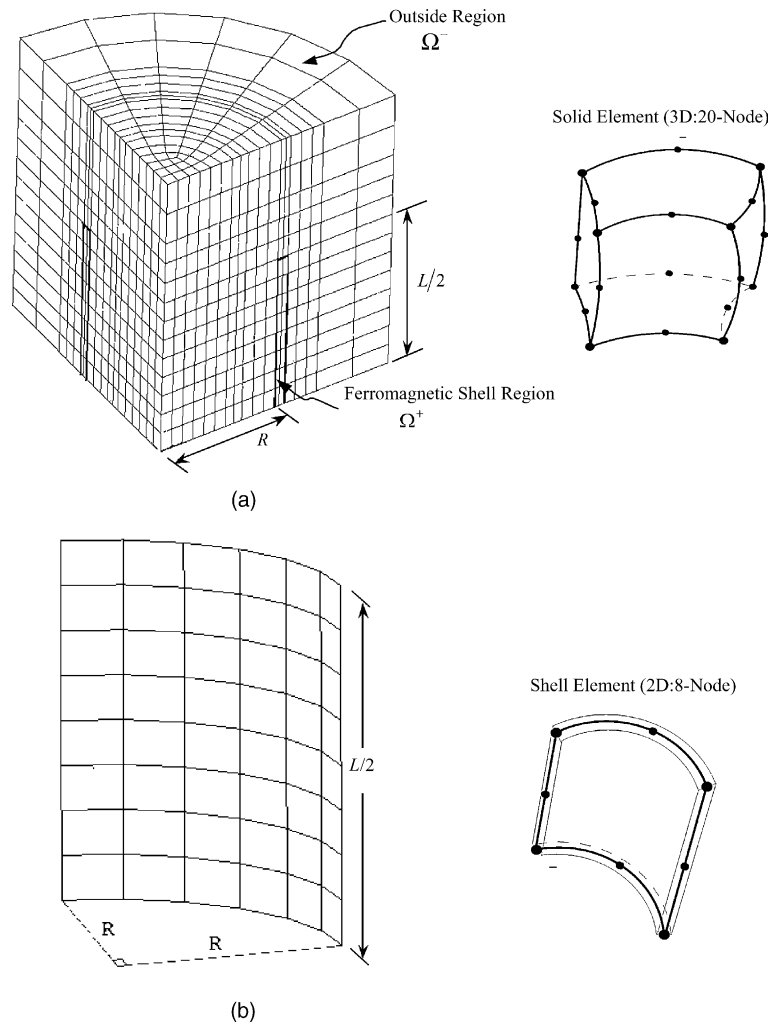
Fig. 3. The finite element meshes for magnetoelastic shell analysis: (a) magnetic field analysis and (b) deformation field analysis for cylindrical shell.

being satisfied, finally, the magnetoelastic solution $[\mathbf{U}] = \lim\limits_{m \to \infty} [\mathbf{U}]_m$ of the deformation for ferromagnetic shell under an applied magnetic field $\mathbf{B}_0$ can be obtained. Here, $\| \cdot \|$ is defined the infinite vector norm, m is the number of iterations and $0 < \varepsilon \ll 1$ denotes a prescribed limit.

It is obviously that above iteration process is sensitive to the initial displacement $[\mathbf{U}]_0$ of the shell. In order to improve the convergence of iteration, we make the magnitude of the applied magnetic field $\mathbf{B}_0$ increase step-by-step, and take the iterative initial displacement $[\mathbf{U}]_0$ for a given magnetic field $\mathbf{B}_0$ as the one for the last applied magnetic field $\mathbf{B}_0 - \Delta\mathbf{B}_0$. The validity of this method is confirmed in our numerical simulation.

5. Numerical results and discussions

In this section, two kinds of experiments conducted by Moon (1984) and Miyata and Miya (1988) are respectively simulated with the theoretical mode and FEM computation program proposed in this paper.

Table 1
Material and geometric parameters for experiments

Parameter	Miyata and Miya's experiment (1988)	Moon's experiment (1984)
Length L (mm)	80	76
Radius R (mm)	15	12.7
Thickness h (mm)	0.5	0.254
Young's modulus Y (MPa)	2.15×10^5	2.0×10^5
Poisson's ratio v	0.3	0.3
Relative permeability μ_r	1000	10,000

All material and geometric parameters for these two kinds of experiments used by the authors are adopted in our numerical program and given in Table 1. Since it is not easy to simulate the end constraints of the cylindrical shell in Moon's experiment, here, we will take Miyata and Miya's experiment as an example to verify the theoretical model suggested in this paper. Then, by introducing the effect of an elastic constant of the end constraints on the stresses of the cylindrical shell, we calculated the magnetoelastic stress of ferromagnetic shell used in Moon's experiment and tried to give a reason why there exhibited the discrepancies between Moon's predicted results and his measured ones.

Firstly, for the convergence and verification of the coupled FEM of magnetic field and deformation of ferromagnetic shell, two finite element meshes were used for the magnetic field and shell. One having 2880 magnetic elements and 13,481 points (the corresponding shell elements being of 64 and points of 225), and another having 3344 magnetic elements and 15,577 points (the corresponding shell elements being of 80 and points of 277) are examined for the evaluations magnetic force and displacement of the cylindrical shell as a typical mesh presented in Fig. 3. For the magnetic force distribution and displacement of shell, the difference in the results between two meshes varied in change of 1–3%. The results in this paper were generated from the second mesh scheme.

Secondly, with adopting the geometrical and material parameters of Miyata and Miya's experiment, we respectively calculated the equivalent normal and tangential (i.e., the direction in θ) magnetic forces given by several theoretical models for a cylindrical thin shell before the shell deforms. The distributions of magnetic forces are plotted in Fig. 4a–d. It is obvious that the distributions of the magnetic forces given by Eqs. (17), (23), (26) and (29) are different, which will lead to the different predictions on the strain of the cylindrical shell. The circumferential bending strain versus angle for the cylindrical shell is plotted in Fig. 5, in which the angle θ is from 0° to 90° because of the symmetry of shell. From Fig. 5a, it can be found that the theoretical results got by the model and the numerical program suggested in this paper are in good agreement with Miyata and Miya's measured data. The relative errors are, respectively, 22.4% at $\theta = 0°$ and 15.1% at $\theta = 90°$, lower than Miyata and Miya's ones which are 40% at $\theta = 0°$ and 34.2% at $\theta = 90°$, respectively. Therefore, the model and the program suggested in this paper are effective to describe the magnetoelastic problem of soft ferromagnetic structures in magnetic field. In Fig. 5b, we plot the circumferential bending strain versus the magnetic field intensity B_0^2 for different θ, which shows that the deformation is almost proportional to a squared applied magnetic-field intensity, and the strain at $\theta = 0°$ increases fast with an increasing magnetic-field intensity B_0 so that more attention should be paid to due to high stress even for a small applied field. With the aid of the numerical program, the circumferential bending strains of the cylindrical shell taken by Miyata and Miya in their experiment are also calculated by the Moon–Pao's model (i.e., Eq. (23)), the Pao–Yeh's model (i.e. Eq. (26)) and the Eringen–Maugin's model (i.e. Eq. (29)), respectively. The circumference stains at $\theta = 0°$ and 90° as well as the relative errors between the predicted result and the measured one list in Table 2. From Table 2, it is can be found that the predicted results given by this paper's model are in better agreement with the experiment data than that given by other models.

For the Moon's model (1984), it should be got a good prediction for the cylindrical shell according to the discussion given in Section 3 since the magnetic permeability of soft ferromagnetic materials μ_r usually is
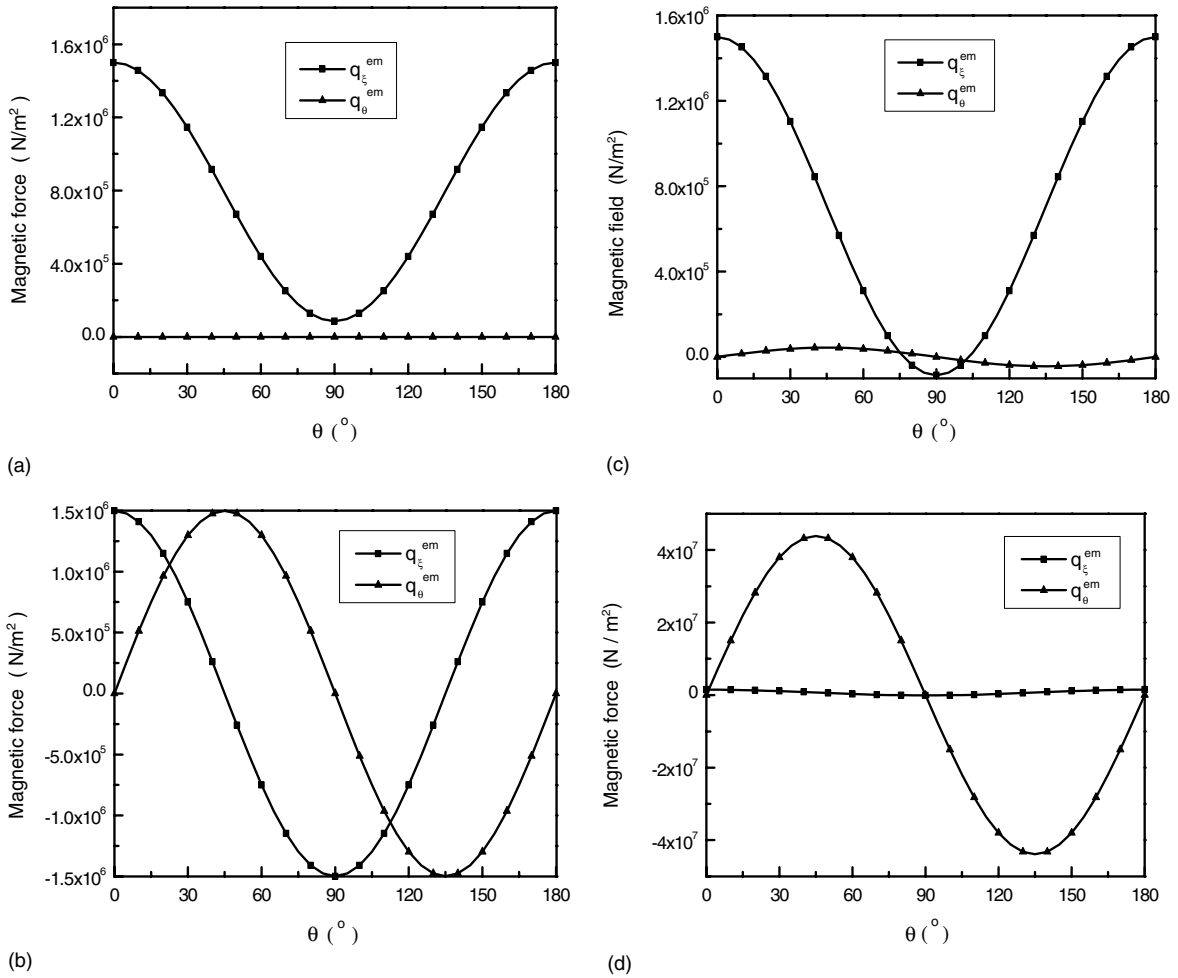
Fig. 4. The distribution of equivalent magnetic force in circumference ($z = L/2$, $B_0 = 1.0$ T): (a) the model in this paper, (b) Moon–Pao's model, (c) Pao–Yeh's model and (d) the Eringen–Maugin's model.

greatly high. Fig. 6 plots the magnetic forces respectively from Eqs. (17) and (30) along with the relative permeability μ_r of soft ferromagnetic material, which displays there is almost no difference between two models for the case $\mu_r > 10^4$. However, the predicted maximum stress at 0.05 T, given by Moon (1984), was 990 N/cm^2 and the measured stress was 520 N/cm^2. We try to analyze the discrepancy from two hands. On the one hand, we firstly calculate the distribution of the magnetic force at $\theta = 90°$ in the length z of the shell, shown in Fig. 7. It is clear that the magnetic forces at the ends are larger than those in the middle part of the shell. So, it may not be reasonable to treat a finite-length cylindrical shell as an infinite one. On the other hand, since the cylindrical shell in Moon's experiment was supported at its ends by circular nylon plates, we introduce an elastic constant K based on the Winkler's model into the boundary conditions in which the cylindrical shell was not clamped or simply supported ($K \to \infty$) and also not free ($K \to 0$). The circumferential strains at different angles for a given magnetic field $B_0 = 0.05$ T and several cases of the elastic constant K are shown in Fig. 8. From Fig. 8, one can find that the effect of the end constraint on the deformation of the cylindrical shell is obvious. When $K = 3.0 \times 10^3$, the strain is about 500 N/cm^2, which is very close to Moon's measured one.
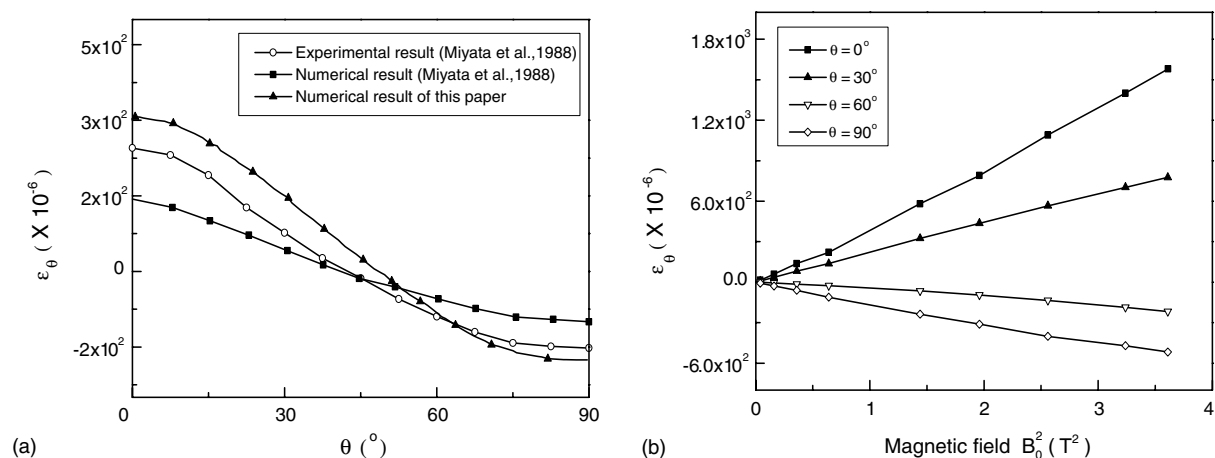
Fig. 5. Circumferential bending strain for a cylindrical shell in a magnetic field ($z = L/2$): (a) circumferential bending strain versus angle ($B_0 = 1.0$ T) and (b) circumferential bending strain versus magnetic field.

Table 2
The circumferential strain at the middle section of a ferromagnetic cylindrical shell in magnetic field ($B_0 = 1.0$ T)

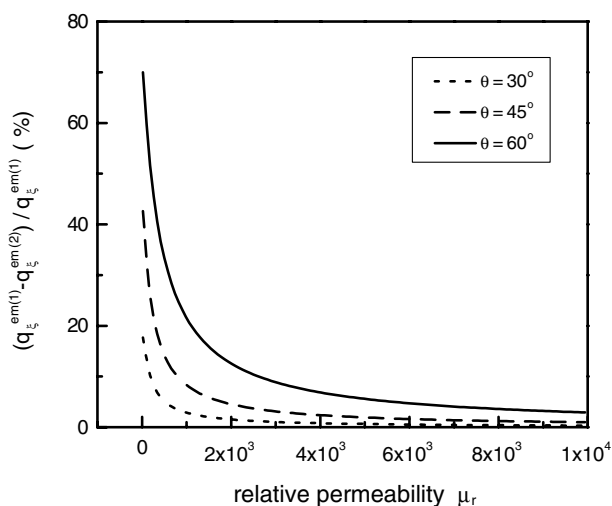| Strain $\varepsilon_\theta (\times 10^{-6})$	Experiment result Miyata and Miya (1988)	This paper result	Moon and Pao (1968)	Pao and Yeh (1973)	Eringen and Maugin (1990)
$\theta = 0°$	250	306	531	397	489
Relative error (%)	–	(22.4)	(112.4)	(58.5)	(95.6)
$\theta = 90°$	−152	−175	−576	−203	−7134
Relative error (%)	–	(15.1)	(278.9)	(33.6)	(4593.4)

Fig. 6. The relative difference of magnetic force between this paper's model $q_\xi^{em(1)}$ and Moon's model $q_\xi^{em(2)}$ versus the magnetic permeability μ_r ($B_0 = 0.05$ T).
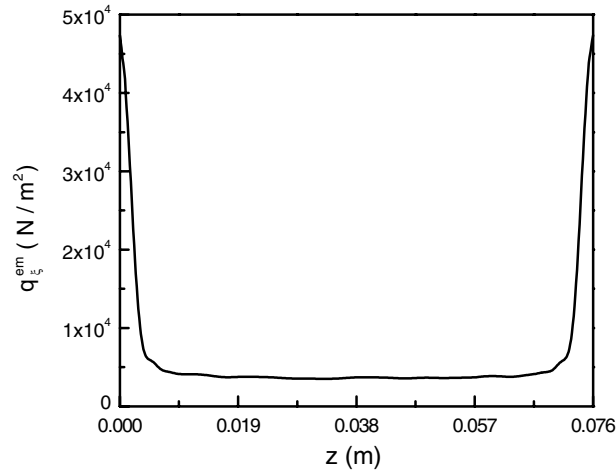
Fig. 7. The distribution of the magnetic force in the length ($B_0 = 0.05$ T, $\theta = 90°$).
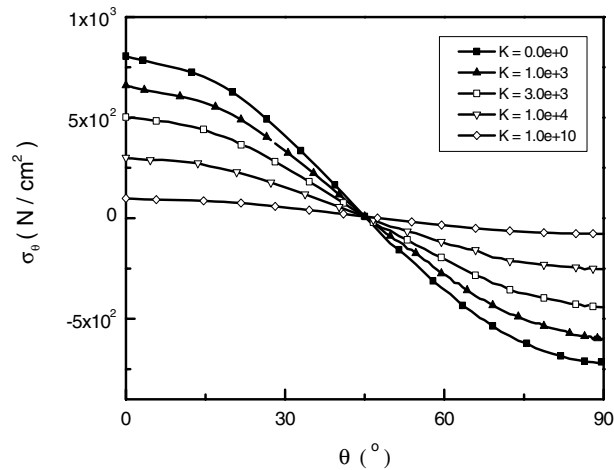

Fig. 8. Circumferential bending strain for different elastic constant K ($z = L/2$, $B_0 = 0.05$ T).

6. Conclusions

In this paper, an expression of equivalent magnetic forces exerted on a soft ferromagnetic shell in a magnetic field is derived by a variational principle. This expression not only can be used to describe the magnetoelastic buckling of a magnetoelastic plate in a uniform transverse magnetic field, but also can be used to describe the magnetoelastic vibrating of a magnetic plate in a uniform in-plane magnetic field, which cannot be realized by other existing models. A computation formulation combined the finite element method with the iterative method is suggested to calculate the deformation of the cylindrical shell. The numerical simulation for the cylindrical shell, which was experimentally measured by Miyata and Miya (1988), shows that our predictions on the circumferential strains are in good agreement with the experimental data. In

addition, the Moon's model (1984), which was used to predict the stress of the shell, is studied in this paper. It is found that there is almost no difference between the Moon's model and the model suggested in this paper when the magnetic permeability $\mu_r > 10^4$. The discrepancy between the theoretical results given by Moon (1984) and his experimental data is from the simplification of the infinite-length cylindrical shell for the finite-length one and the effect of the end constraints of the cylindrical shell.

Acknowledgements

References

Eringen, A.C., Maugin, G., 1990. In: Electrodynamics of Continua, vol. 1. Springer-Verlag, New York.

Miyata, K., Miya, K., 1988. Magnetic field and stress analysis of saturated steel. IEEE Trans. Magn. 24, 230–233.

Moon, F.C., 1984. Magneto-solid Mechanics. Jone Wiley and Sons, New York.

Moon, F.C., Pao, Y.H., 1968. Magnetoelastic buckling of a thin plate. ASME J. Appl. Mech. 35, 53–58.

Moon, F.C., Pao, Y.H., 1969. Vibration and dynamic instability of a beam-plate in a transverse magnetic field. J. Appl. Mech. 36, 92–100.

Pao, Y.H., Yeh, C.S., 1973. A linear theory for soft ferromagnetic elastic solids. Int. J. Engng. Sci. 11, 415–436.

Takagi, T., Tani, J., Matsubara, Y., Mogi, I., 1993. Electromagneto-mechanics coupling effects for non-ferromagnetic and ferromagnetic structures. In: Miya, K. (Ed.), Proceedings of the Second International Workshop on Electromagnetic Forces and Related Effects on Blankets and Other Structures Surrounding Fission Plasma Torus, September, Japan, pp. 81–90.

Timoshenko, Woinowsky-Krieger, 1959. Theory of Plates and Shells. McGraw-Hill.

Zheng, X.J., Zhou, Y.H., Wang, X.Z., Lee, J.S., 1999. Bending and buckling of ferroelastic plates. ASCE J. Eng. Mech. 125, 180–185.

Zhou, Y.H., Miya, K., 1998. A theoretical prediction of natural frequency of a ferromagnetic beam plate with low susceptibility in an in-plane magnetic field. ASME J. Appl. Mech. 65, 121–126.

Zhou, Y.H., Zheng, X.J., Miya, K., 1996. Magnetoelastic bending and snapping of ferromagnetic plates in oblique magnetic fields. Fusion Eng. Des. 30, 325–337.

Zhou, Y.H., Zheng, X.J., 1997. A general expression of magnetic force for soft ferromagnetic plates in complex magnetic fields. Int. J. Engng. Sci. 35, 1405–1417.